ARTICLE

Degradation of Alkaline Lignin in the Lactic Acid-Choline Chloride System under Mild Conditions

Penghui Li[1,2], Zhengwei Jiang[2], Chi Yang[2], Jianpeng Ren[1,2], Bo Jiang[1,2] and Wenjuan Wu[1,2,*]

[1]Jiangsu Co-Innovation Center of Efficient Processing and Utilization of Forest Resources, Nanjing Forestry University, Nanjing, 210037, China

[2]College of Light Industry and Food Engineering, Nanjing Forestry University, Nanjing, 210037, China

[*]Corresponding Author: Wenjuan Wu. Email: wenjuanwu@njfu.edu.cn

ABSTRACT

Lignin is a natural polymer, second only to cellulose in natural reserves. Degradation is one of the ways to achieve the high-value transformation of lignin. Deep eutectic solvent (DES) thermal degradation of lignin can be used as an excellent green degradation method. This paper introduces the degradation mechanism and effect of the lactic acid-choline chloride DES system in dissolving and degrading alkaline lignin, and the final solvent recovery. It can also be found from the scanning electron microscope (SEM) images that the surface of the degraded solid product is transformed from smooth to disordered. Fourier transform infrared (FTIR) spectroscopy and ^{1}H-NMR spectroscopy were used to characterize the changes in lignin functional groups during DES treatment. The results showed that the content of phenolic hydroxyl groups increased after degradation, indicating that the β-O-4 ether bond was broken. The molecular weight of the degraded lignin was observed by gel permeation chromatography (GPC), and the lignin residue with low molecular weight and narrow polydispersity index was obtained. The lowest average molecular weight (Mw) reached 2512 g/mol. The ratio of oxygen to carbon atoms in lignin increased substantially during degradation as measured by X-ray photoelectron spectroscopy (XPS), probably because DES treatment was accompanied by many oxidation reactions, which led to significant structural changes in lignin and a large number of ether bond breakage reactions during the reaction. The main final degradation products are aromatic monomers, vanillin, butyrovanillone, etc.

KEYWORDS

Lignin; mild conditions; deep eutectic solvents (DES); degradation mechanism

1 Introduction

Due to the increasing depletion of fossil fuels and the increasingly prominent global climate change problem, the search for renewable alternative energy has been imminent [1]. To advance the circular economy and environmental sustainability worldwide, it is inevitable to develop green energy and extract value-added chemicals and materials from biomass [2]. Lignocellulosic biomass can be a potential substitute for fossil raw materials to improve global warming [3]. It is mainly composed of three parts, lignin, cellulose and hemicellulose. Among them, alkaline lignin (AL) accounts for 85% of global lignin production. It is the main by-product of the paper industry, which is generally discarded or used as fuel,

resulting in waste of resources and environmental pollution [4,5]. The macromolecular structure of lignin is a three-dimensional structure composed of three main phenylpropane monomers (*p*-coumarol, coniferyl alcohol and sinapyl alcohol) connected by carbon-carbon bonds and carbon-oxygen bonds. They are linked differently, of which β-*O*-4 bonds are the most abundant in natural lignin [6]. Lignin is a renewable resource with the highest content of benzene rings in nature, and it is also the most abundant phenolic compound, so it has the prospect of being converted into aromatic monomer chemicals. At present, how to effectively degrade lignin into small molecular compounds is one of the most popular works [7].

The degradation of lignin using conventional methods often involves more demanding reaction conditions (e.g., reaction temperature of 360°C, H_2 pressure of 70 bar, and catalyst Raney Ni) [8]. DES is considered as a green alternative to conventional organic solvents, most of which are volatile, flammable and toxic [9]. In contrast, DES is renewable, simple to prepare, has mild reaction conditions and has good solubility to lignin. These excellent properties have contributed to its promising performance in degrading lignin [10]. Among the various types of DES, one of the most classical hydrogen bond acceptors (HBA) used for the preparation of DES is choline chloride (ChCl), since ChCl can be combined with hydrogen bond donors (HBD) such as urea, organic alcohols, and organic acids to form DES [11]. Based on the binding mechanism of HBD and HBA, DES can provide mild reaction conditions and acid-base catalysis to lead to the cleavage of the unstable ether bond between the phenyl propane units, which is the desired result [12]. DES can degrade lignin well, Li et al. [13] used a DES system composed of choline chloride and *p*-toluenesulfonic acid to degrade lignin. The ether bonds in lignin were selectively broken during the degradation process, and the phenolic hydroxyl groups were also increased. Wang et al. [14] designed a temperature-responsive DES to degrade lignin, in which the catalytic performance of [Bmim] Cl-EDTA was better than that of other DES. Finally, the degradation rate of lignin reached 83.63%, and the solvent could be recycled as well. After 4 cycles, the degradation rate of lignin still did not change significantly.

Tan et al. [15] used choline chloride/lactic acid to form a DES system to extract lignin, and finally obtained many small molecules through depolymerization, including most phenolic compounds. The oxidation of the hydroxyl group to the carboxyl group is more efficacious [16]. Similarly, Wang et al. [17] used a lignin model compound in a choline chloride/lactic acid DES system. They found that DES could effectively cleave the β-*O*-4 bond with a decrease in product molecular weight and an increase in hydroxyl groups, indicating that the reaction principle of this DES system was almost the same as that of HCl-catalyzed lignin degradation. Shen et al. [18] treated bienzymatic lignin isolated from eucalyptus with DES (ChCl/lactic acid), where β-*O*-4 base cleavage increased phenolic OH. By contrast, dehydration or acylation reactions resulted in a decrease in aliphatic OH. At high temperatures, aryl-ether and carbon-carbon bonds are broken, leading to a decrease in molecular weight. Herein, we concluded that lignin was also well degraded in the DES of choline chloride-lactic acid. To validate this hypothesis, we described the bond-breaking effect of acidic DES prepared by choline chloride and lactic acid on alkaline lignin to explore the degradation mechanism.

2 Experiment

2.1 Materials

The lignin material was purchased from a Nanjing pulp and paper mill (China). The elemental compositions in the dried lignin were 64.55 wt% carbon, 5.40 wt% hydrogen, 1.70 wt% sulfur and 0.11 wt% nitrogen (measured by the Elementar Vario EL cube analyzer, Germany). The number-average and weight-average molecular weight of the alkaline lignin were 1743 and 6483, respectively, and the polydispersity was 3.719 (determined by the Gel Permeation Chromatography instrument LC-20A with eluent tetrahydrofuran, Japan). Choline chloride, lactic acid and other chemicals were purchased from Sinopharm Chemical Reagent Co., Ltd. (China) without further purification.

2.2 Procedure for Degradation of Lignins

The aqueous compound of choline chloride and lactic acid is stirred at 100°C for about 30 min according to the molar ratio of 1:1 (the molar ratio of other types of DES is determined according to the actual situation) to form a colorless and transparent solution, which is stored in a dryer.

Add 1 g lignin and 19 g DES into the reaction flask to make the mass fraction of lignin 5%. Add 250 μL distilled water and heat for different times under the conditions of 90°C, 110°C, 130°C, 150°C, 170°C and 180°C. After the reaction, remove the reaction flask and immediately submerge it in a cold water bath to end the reaction. Lignin was precipitated by adding 50 mL of acidic water (pH = 2) to the reaction flask, centrifuged, and the supernatant was collected with the solid, after which the lignin was washed three times with about 100 mL of distilled water. Sixty mL of the supernatant was extracted by 300 mL of toluene. The mixture was partitioned to obtain the organic phase. Subsequently, toluene was removed by rotary evaporation at 40°C to acquire lignin oil. The supernatant was evaporated by vacuum rotary evaporation to remove water to obtain the recovered deep eutectic solvent. The obtained solid was frozen for 24 h and freeze-dried for 48 h (one shown in Fig. 1). The lignin degraded for 3, 5, 7, 9 and 13 h is labeled severally.
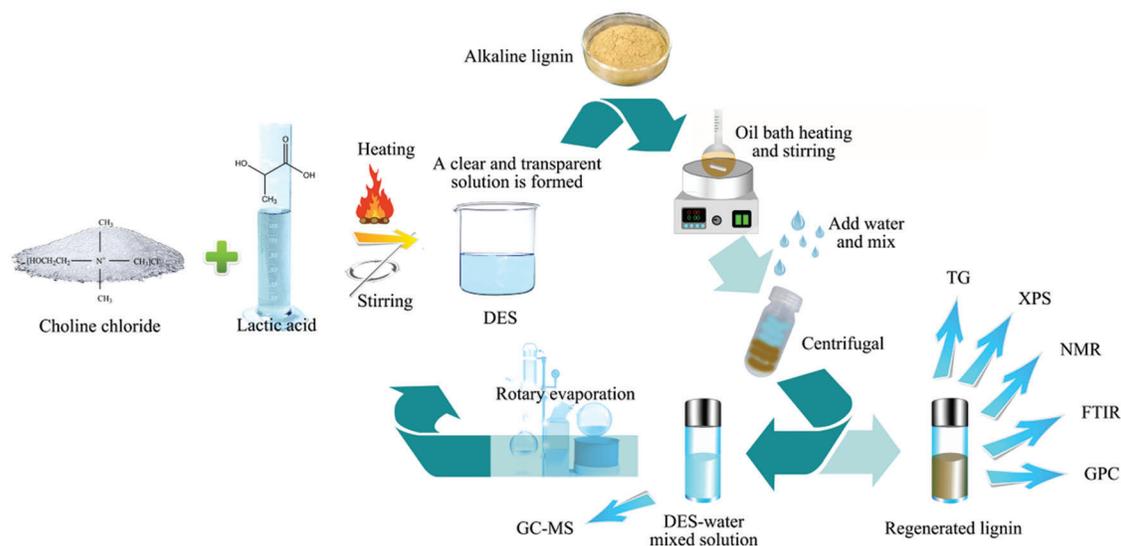
Figure 1: The scheme of degradation of lignin in deep eutectic solvent

2.3 Characterization and Analysis of the Products

To examine the morphology of the solid products, scanning electron microscope (SEM) measurements were performed by FEI Scios 2 HiVac field emission scanning electron microscopy (FEI, USA). Weigh 10 mg of dry lignin product, dissolve it in slightly alkaline water, add FC reagent, make up to volume, add 20% Na_2CO_3 after 5 min, and then make up to 50 mL. After the mixture was stirred for 2 h, the absorbance of lignin and regenerated lignin at 760 nm was measured using an ultraviolet spectrophotometer (TU-1900, China) to obtain the content of phenolic hydroxyl groups in the lignin samples.

The structure and functional groups of the products were examined by Fourier transform infrared spectroscopy (FTIR) on a VERTEX 80V FTIR spectrometer (Bruker, Germany). The scanning range was 400–4000 cm^{-1}, and the scan number was 32. Acetylation of lignin prior to molecular weight testing [19]. The gel permeation chromatography determined the molecular weight and dispersion of lignin samples (SHIMADZU LC-20A, Japan). The concentration of lignin in tetrahydrofuran (THF) was about 5 mg/mL. The column temperature was 40°C, THF was the eluent, and the flow rate was 1 mL/min. The

average molecular weight of lignin was measured by an external standard method, in which monodisperse polystyrene was applied as the standard compound.

Hydrogen spectra with 2D ^{13}C-^{1}H HSQC (heteronuclear single quantum correlation) spectra were obtained at room temperature using a 600 MHz fully digital superconducting NMR spectrometer (Bruker Biospin AVANCE III HD, Switzerland). ^{1}H NMR was acquired by dissolving 12 mg of acetylated lignin sample in 0.5 mL of deuterated dimethyl sulfoxide and shaking to dissolve it. The ^{1}H spectral range was 0–16 ppm (9615 Hz) with 2048 sampling points in the ^{1}H dimension and a relaxation time of 1.5 s, accumulated 64 times. For the 2D NMR acquisition, 50 mg of lignin sample was weighed and dissolved in 0.5 mL DMSO-d6, and the signal was acquired using the HSQC spectral counterpart. The spectral widths in the ^{1}H and ^{13}C dimensions were 0–16 ppm (9615 Hz) and 0–165 ppm (24900 Hz), respectively. The hydrocarbon coupling constant is 145 Hz, and the number of sampling points in the ^{1}H dimension is 2048 with a relaxation time of 1.5 s. The number of sampling points in the ^{13}C dimension is 256, totalling 64 times. The total test time was 22 h with zero-punching before Fourier transform.

The thermal properties of lignin before and after degradation were determined employing a thermogravimetric analyzer (STA449F5 Jupiter, Germany). The heating rate was 10 °C/min, ranging 30°C–800°C, and the flow rate of high-purity N_2 was 20 mL/min. The small molecule degradation products of lignin were analyzed by gas chromatography-mass spectrometry (Thermo Scientific ISQ 7000, USA). The Rxi-5ms column (30 m × 0.25 mm × 0.25 μm) was used. The carrier gas was helium at a flow rate of 1.4 mL/min. The column temperature was maintained at 50°C for 1 min, increased to 300°C at a rate of 10°C/min, maintaining at 300°C for 10 min. The injection volume was 1 μL, the temperature was 280°C and the diversion ratio was 30:1. The peaks were assigned based on a comparison with the National Institute of Standards and Technology (NIST, 2005) mass spectrometry library. An XPS spectrometer (Thermo Scientific K-Alpha, UK) with a chamber vacuum better than 5.0×10^{-7} mBar and an Al Kα-ray (hv = 1486.6 eV) energy analyzer with fixed transmission energy of 100 eV and step size of 1.00 eV was used to test the X-ray photoelectron spectra of the samples.

The phenolic hydroxyl content of lignin and its degradation products was determined by the Folin-Ciocalteu method (FC method) [20,21]. The content was measured by this method using vanillin as a standard substance to determine phenolic hydroxyl content. The regression equation was made based on the relationship between the absorbance of phenol at 760 nm and the concentration (c, μmol/L): y = 0.0138x + 0.00076 (correlation coefficient R^2 = 0.9988) (as shown in Fig. 2).
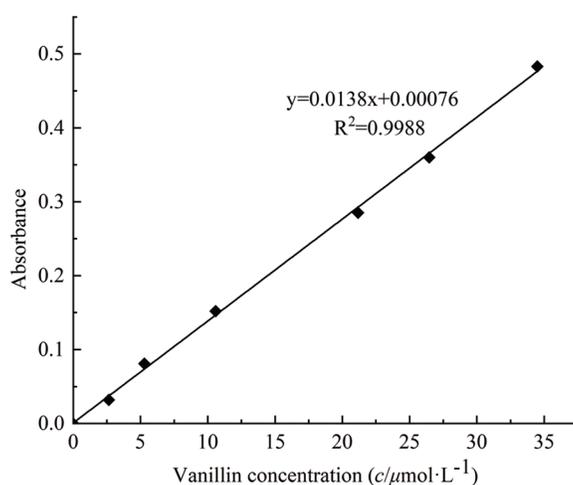
Figure 2: Relationship between vanillin concentration and absorbance in solution

The regenerated lignin yield of lignin was calculated according to Eq. (1) [22,23].

$$\text{Regenerated lignin yield} = \frac{m}{m_0} \times 100\% \qquad (1)$$

where m_0 and m denote the mass of lignin before degradation (g) and the mass of regenerated lignin after degradation by centrifugation and filtration (g), respectively.

3 Results and Discussion

3.1 SEM Morphology Analysis

Fig. 3 shows the SEM images of proto-lignin and solid products at different reaction times. The surface of the raw lignin is smooth. In contrast, the surface of the degraded solid product is more disordered [24].

It can be observed by SEM images that the resultant DES degradation produced more uniform lignin fragments, indicating that the DES degradation significantly reduced the molecular weight of lignin. It can be seen that the dispersion of lignin decreases after wood degradation, which is consistent with the GPC results. This also confirms the regeneration of homogeneous lignin subunits with reduced molecular weight after DES degradation through dissociation or degradation processes [18].
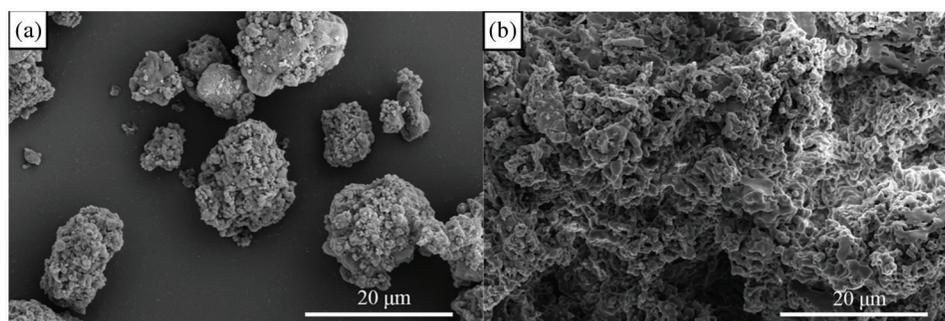
Figure 3: Scanning electron micrographs of the original alkaline lignin (a) and the regenerated lignin (b)

3.2 Effect of the Reaction Temperature

Some physical properties of DES are easily affected by temperature, and the viscosity of DES decreases with increasing temperature, thus improving heat and mass transfer [25]. Based on this, we investigated the effect of depolymerization of lactic acid-based DES at 90°C, 110°C, 130°C, 150°C, 170°C, and 180°C when the reaction time was 7 h (as shown in Fig. 4). At lower temperatures (e.g., 80°C), the depolymerization products are less and the phenolic hydroxyl content is naturally lower. As the temperature increases, the β-O-4′ bond in lignin breaks and the type and content of lignin monomer products increase (with a sharp increase in phenolic OH content), along with the formation of aromatic oligomers, indicating that higher temperatures favor the depolymerization of lignin [26]. Meanwhile, the recovery of regenerated lignin decreased with increasing reaction temperature. The relatively low yield of regenerated lignin samples at a higher temperature (180°C) implies that some of the lignin fractions depolymerized into small fragments after DES treatment and could not be precipitated as regenerated lignin.
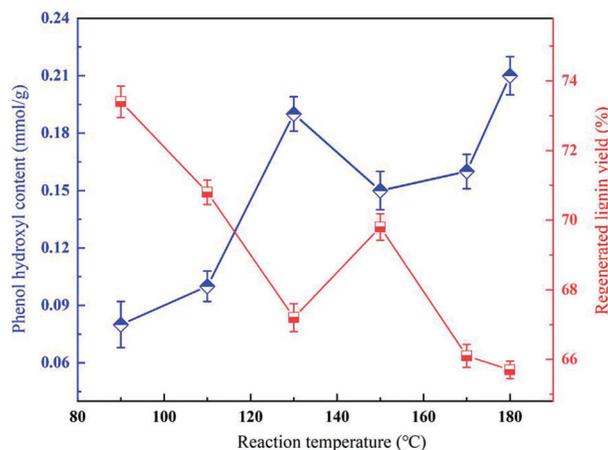
Figure 4: Yield of lignin and phenolic hydroxyl content of supernatant at different reaction temperatures

3.3 Effect of the Reaction Time

Following the optimal experimental conditions at different reaction temperatures, we also considered the effect of reaction temperature on it. We set different reaction times, such as 3, 5, 7, 9, 11 h, at the reaction temperature of 180 °C, to examine the effect of varying reaction times on lignin depolymerization. It can be seen from Fig. 5 that the phenol content of lignin increases slightly with extending reaction time. However, at a long reaction time, the regenerated lignin may undergo polycondensation [13]. The following characterizations are based on the original alkaline lignin and the regenerated lignin with a reaction temperature of 180 °C and a reaction time of 7 h.
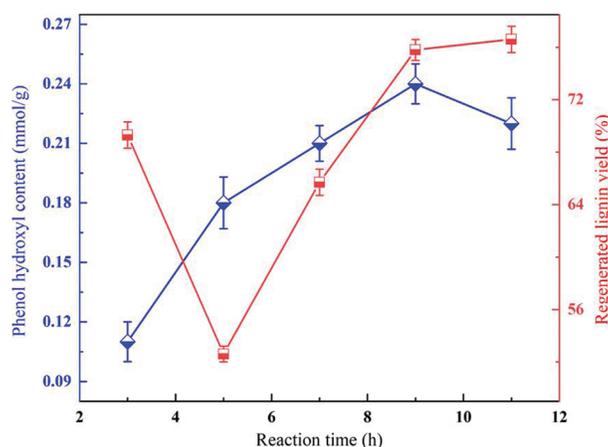
Figure 5: Yield of lignin and phenolic hydroxyl content of supernatant at different reaction times

3.4 GPC Analysis

In order to study the effect of deep eutectic solvent treatment on the molecular weight of lignin, GPC was used to detect the molecular weight of acetylated lignin before and after degradation. It can be seen from Table 1 that the M_W of degraded lignin is between 2512–4793 g/mol, which is lower than the M_W value of raw alkaline lignin (6483 g/mol). It is generally believed that the less the aryl ether bond content in lignin, the smaller the molecular weight. The smaller the condensation structure, the smaller the molecular weight. Combined with the results of infrared and nuclear magnetic analysis, with the extension of reaction temperature, the content of ether bonds in lignin gradually decreased. In contrast, the molecular weight of lignin firstly decreased and then increased, indicating that lignin depolymerized, broken ether bond and condensation in the acidic deep eutectic solvent [27]. The increase in

polydispersity coefficient (M_W/M_n) from 2.208 at 110°C to 2.737 at 150°C is also evidence of condensation reactions, which increase the recalcitrance and heterogeneity of the resulting lignin upon repolymerization [28]. Acidic conditions can trigger the formation of positive carbon ions through proton-induced elimination of lactic acid from the benzyl position, which can lead to the β-ether bond's breakage, thereby reducing the molecular weight [29]. In addition, the M_W/M_n of the regenerated lignin after degradation with DES was lower (1.83–2.74) compared to alkaline lignin, indicating the formation of a more homogeneous lignin structure. This shows that a homogeneous and relatively low molecular weight lignin can be obtained after DES treatment.

Table 1: Molecular weight and polydispersity coefficient of lignin before and after degradation

Reaction conditions	M_w	M_n	M_w/M_n
Alkaline lignin	6483	1743	3.719
90°C CC-LA	4066	1748	2.326
110°C CC-LA	4103	1858	2.208
130°C CC-LA	4209	1790	2.351
150°C CC-LA	4305	1573	2.737
170°C CC-LA	3238	1386	2.336
180°C CC-LA	2512	1375	1.827

Note: CC, Choline chloride; LA, lactic acid.

3.5 FT-IR Analysis

For the purpose of comparing the structural changes of lignin before and after degradation, the IR spectra of the regenerated lignin obtained from the degradation of alkaline lignin feedstock and lactic acid-based DES were characterized (as shown in Fig. 6). It was found that there were some apparent differences between IR spectra of degraded lignin and alkaline lignin, such as the absorption peak changed near 1602 and 1508 cm^{-1}, representing the aromatic skeleton vibration of lignin, 1416 cm^{-1} corresponding to the CH deformation combined with the aromatic ring vibration, indicating that the aromatic ring structure of lignin was partially destroyed during the deep eutectic solvent treatment. Comparing the absorbance of the characteristic absorption peak of the benzene ring at 1508 cm^{-1} before and after DES treatment with that of 1508 cm^{-1}, it can be found quantitatively that the content of benzene ring functional groups in lignin was reduced [13]. The intensity of the 3420 cm^{-1} absorption peak of hydroxyl stretching vibration absorption of lignin decreased slightly after treatment. In comparison, the intensity of 1037 cm^{-1} absorption peak representing the C-O deformation vibration of secondary alcohols and aliphatic esters weakened substantially, presumably due to the breakage of the ether bond in the lignin molecule during the treatment with deep eutectic solvents and the new condensation reaction, lignin degradation reaction competed with the condensation reaction [30]. This is presumably due to the breakage of the ether bond in the lignin molecule during the deep eutectic solvent treatment and the new condensation reaction, where the lignin degradation reaction competes with the condensation reaction [30]. The peak intensity of the degraded lignin (CH stretching of methyl and methylene groups) was slightly decreased at 2930 cm^{-1}, which implies that lactic acid-based DES treatment may lead to demethoxylation reactions. The absorption peak near 1735 cm^{-1} (non-conjugated ketone carbonyl and carboxycarbonyl) observed to appear in regenerated lignin is significant. It is possible that the acidic DES treatment led to the breakage of the β-O-4 bond, resulting in the appearance of the non-conjugated carbonyl group, and then possibly the formation of the Hebert ketone [31]. As proposed by Wang et al. [17], in the reaction pathway of acidic DES, the β-O-4 bond in lignin was broken, and monoketone compounds with non-conjugated

carbonyl groups were also found. Another reason is that with the COOH group in lactic acid and the OH group in the γ-position of lignin between them also an esterification reaction may occur [32]. In addition, the signal at 1024 cm^{-1} (in-plane deformation of aromatic CH) gradually became weaker after lactic acid treatment, indicating that the condensation reaction prevented the in-plane deformation of aromatic CH. The results suggest that DES treatment can destroy the lignin structure. However, the complex transformation of the lignin structure needs to be further confirmed by NMR spectroscopy.
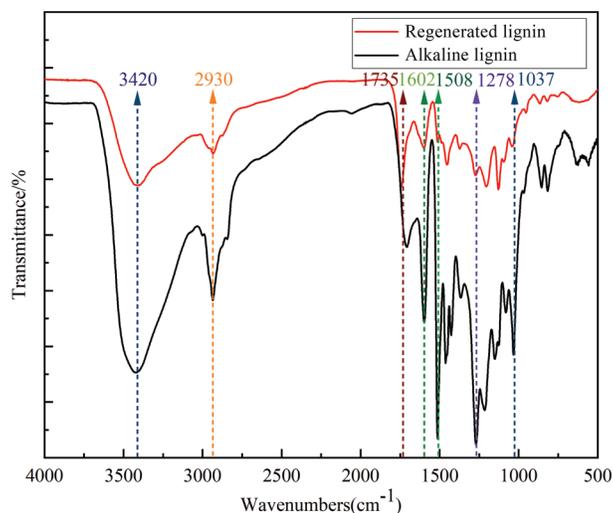
Figure 6: FTIR spectroscopy of the original alkaline lignin (a) and the regenerated lignin (b)

3.6 XPS Analysis

Four types of valence states of C1s on the lignin surface, namely C1, C2, C3 and C4, represent different ways of carbon bonding on the lignin surface. The proportion of C1–C4 in the C1s peaks can be expressed as a percentage of the respective peak areas. There are two types of valence states of lignin O1s, O1, O2 electron-binding energy corresponding to functional groups: O1-oxygen atoms in oxygen-carbon single bonds, such as C-OH, C-O-C; O2-oxygen atoms in carbon-oxygen double bonds, including oxygen atoms in aldehyde, ketone, ester bonds or carbonyl groups, such as C=O, O-C=O [13]. Curve fitting and peak separation were performed for the C1s and O1s of alkaline lignin and acidic deep eutectic solvent treated regenerated lignin. The carbon and oxygen spectra of the X-ray photoelectron spectra were subsequently obtained (Figs. 7a–7d). The results of the lignin oxygen-carbon atomic ratio and the peak area ratio of each carbon and oxygen valence state are listed in Table 2. It can be seen that the O/C atomic ratio of lignin treated with acidic deep eutectic solvent tends to decrease. The relative content of C1 peak increased obviously, probably due to the increase in the carbon-hydrogen or carbon-carbon single bond (which may form a new carbon-carbon bond [13]), the relative content of C2 peak decreased substantially, and the relative content of C3 peak increases visibly. The relative content of C4 peaks increased significantly, presumably leading to the formation of "Hibbert" ketones under acidic conditions, and DES oxidized α-OH groups followed by acylation of γ-OH groups, which facilitated the breaking of ether bonds to produce diketones [33,34]. After degradation, the relative content of O1 in lignin was observably reduced and the relative content of O2 was significantly increased. This indicates that the DES treatment was accompanied by many oxidation reactions, which led to significant structural changes in lignin [16]. Combined with the results of carbon valence analysis, this may be due to the large number of ether bond breakage reactions that occurred in lignin during the reaction [17].
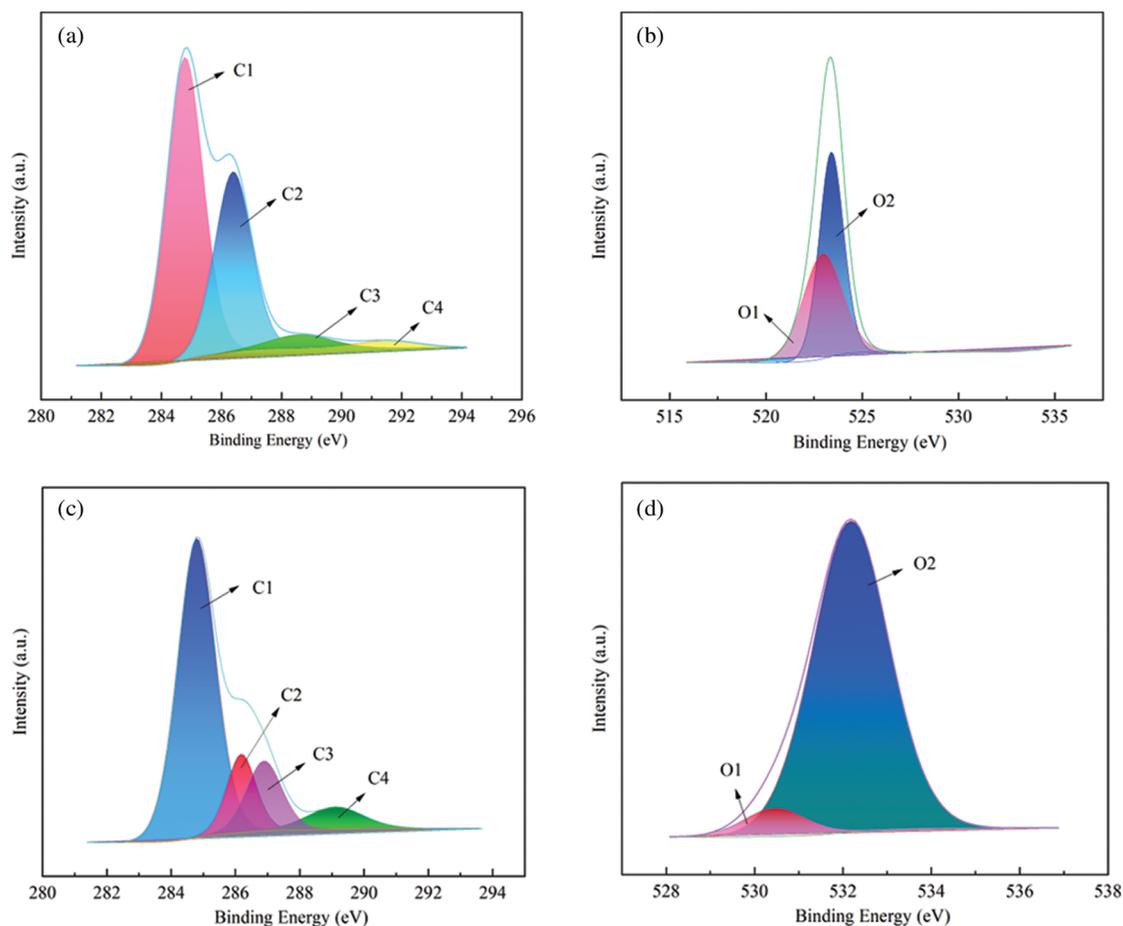
Figure 7: Fitting of C1s and O1s peaks of the original alkaline lignin (a, b) and the regenerated lignin (c, d) with high-resolution XPS spectra

Table 2: Atomic O/C ratios and C1s, O1s peak deconvolution of the original and degraded lignins

	O/C (%)	C1 (%)	C2 (%)	C3 (%)	C4 (%)	O1 (%)	O2 (%)
		C-C, C-H	C-O	O-C-O, C=O	O-C=O	C-OH, C-O-C	C=O, COOR
Alkaline lignin	30.36	57.80	35.26	4.62	2.31	45.36	54.64
180°C CC-LA	24.71	65.36	13.07	7.19	14.38	6.54	93.46

3.7 Thermal Performance Analysis

The TGA curve shows the percentage weight loss of the material relative to the thermal degradation temperature, and the first order derivative (DTG) represents the corresponding weight loss rate. The peak of the DTG curve, DTG max, gives the highest thermal decomposition rate that can be used to compare the thermal stability properties of different materials. The molecular structure of lignin, including the functional groups, branching degree and condensation degree inside the molecule, affects the thermal stability of lignin. In order to further investigate the structure of lignin before and after degradation, the thermal stability of lignin before and after degradation was analyzed, the results are shown in Fig. 8. It can be seen from the TGA curves that the lignin degradation extends over a wide temperature range, i.e.,

175°C–700°C, which indicates several overlapping decomposition steps, as previously observed in the case of woody and non-woody lignin [35]. During the initial stage of thermal degradation (40°C–100°C), the mass loss of lignin is mainly due to water adsorption and the volatilization of small molecules from lignin. As shown in Figs. 8a and 8b, the mass loss rate of regenerated lignin was greater than that of alkaline lignin feedstock at this stage, probably due to the presence of more volatile small molecules in the regenerated lignin, resulting in a greater thermal degradation rate of regenerated lignin at this stage. Within a certain time frame, the longer the reaction time, the more small molecules are present in the regenerated lignin. The rapid thermal degradation stage is 100°C–600°C, in which mass loss mainly occurs, the main products are some organic and phenolic compounds with some gaseous substances. The release of phenolics due to the breakage of C-C bonds between the lignin monomer units is between 357°C–464°C; the decomposition of aromatic rings and guaiacyl/purpurinyl compounds is above 400°C [36]. The maximum degradation rate of alkaline lignin was 3.699%/min, corresponding to the temperature of 411.59°C, while the degraded maximum degradation rate was 5.400%/min (258.37°C). This indicates that the lignin degradation products can be degraded at lower temperatures, which provides a basis for expanding the environmentally friendly development of lignin degradation products. At this stage, the thermal stability of lignin is mainly related to the content of the weakest linkage bond in lignin, the aryl ether bond. It can be found that the thermal stability of lignin decreases substantially at this stage after regeneration by low co-solvent degradation, indicating that the macromolecular structure in lignin depolymerizes after low co-solvent treatment, generating oligomers with relatively low branching, which is consistent with the ^{1}H-NMR spectrum and GPC results. After lactic acid DES treatment, the regenerated homogeneous lignin had moderate aryl ether bonds. It contained aromatic compounds with small molecular weight, which might be the reason for its reduced stability [37]. The "residual char" content of alkaline lignin at 800°C was 39.56%, while the "residual char" content of degraded lignin at 800°C was 39.56%. The decrease in the "residual char" content of degraded lignin at 800°C was presumably due to the decrease in the molecular weight of lignin.
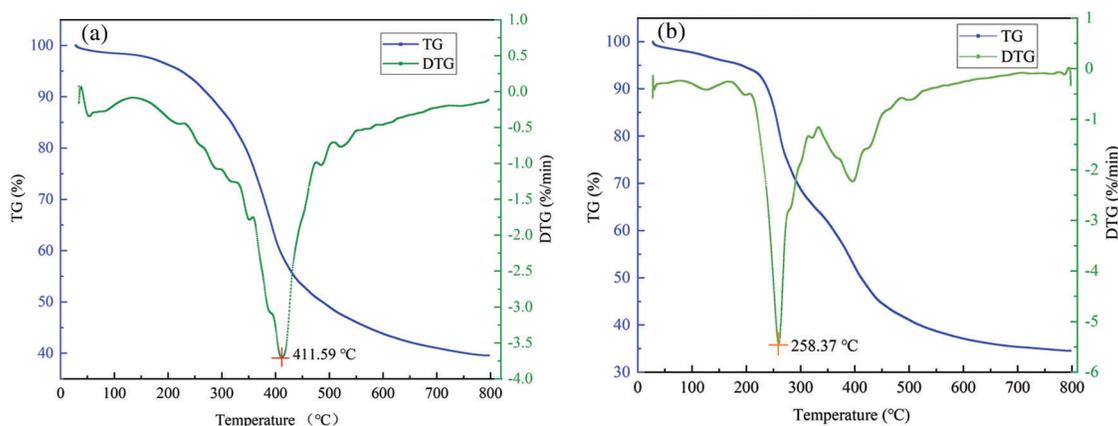
Figure 8: Scanning electron micrographs of the original alkaline lignin (a) and the regenerated lignin after degradation (b)

3.8 ^{1}H-NMR Analysis

Fig. 9 shows the ^{1}H-NMR spectra measured before and after lignin depolymerization. Among them, the aromatic protons of G and S units are observed at signals 7.0 and 6.6 ppm, respectively. 5.0–4.1 ppm is attributed to Hα, Hβ and Hγ signals in the β-*O*-4 structure, 4.2–3.1 ppm is attributed to the H signal of methoxy, and the ratio of G to S is closely related to the methoxy proton (-OCH$_3$), which provides a sharp signal at 3.75 ppm [38]. The sharp peak at 3.5–3.3 ppm is attributed to the proton signal of water

in the solvent. The small peak at 3.4 ppm is attributed to the proton signal in choline chloride, which may be due to a slight reaction between lignin and choline chloride in the solvent or a small amount of deep eutectic solvent remaining in the lignin during the processing. The proton signal at 2.5–2.2 ppm is attributed to the proton signal of aromatic ring acetate and 2.2–1.4 ppm is attributable to the proton signal of aliphatic acetate. It can be seen that the intensity of the acetate signal peak of lignin is significantly higher after degradation. Methoxy can be used as a marker peak to analyze the proton number of each functional group of lignin. It can be inferred that the original lignin has a higher proportion of G units. The degradation products have fewer G, S units and generate a large amount of acetate, which is consistent with the XPS results. Lactic acid has hydroxyl and carboxyl groups, which, under certain conditions, can promote the esterification reaction and lead to the breakage of the β-*O*-4 bond [39].
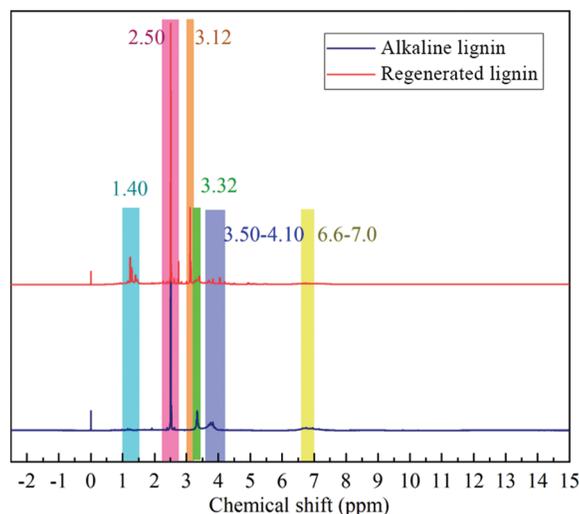
Figure 9: ^{1}H-NMR spectra of original alkaline lignin and the regenerated lignin

3.9 2D-HSQC NMR Analysis

In order to obtain the information about the structure of lignin, we performed two-dimensional carbon-hydrogen correlation spectra on the products before and after lignin degradation, the obtained two-dimensional spectra are shown in Fig. 10. The attribution of main correlation signals in the spectra is shown in Table 3. Four regions can be distinguished on the ^{1}H-^{13}C HSQC spectra of the tested lignin samples: (i) the aliphatic side chain region (δC/δH 50-10/3.0-1.1 ppm); (ii) the aliphatic oxidation region (δC/δH 100-40/6.0-2.5 ppm); (iii) the aromatic/unsaturated region (δC/δH 160-103/8.0-6.0 ppm); (iiii) aldehyde signals (δC/δH 205-190/9.9-9.5 ppm). The aliphatic oxidation region (Figs. 10a and 10c) and the aromatic/unsaturated region (Figs. 10b and 10d) of the HSQC spectra are the most interesting for the study of lignin structure. The signals observed in these regions allow to establish the type of interunit connections and the composition of the phenyl propane unit [40]. As seen in Fig. 10 in the side chain region, a clear methoxy (OCH$_3$) signal appears and only the G-unit signal is present in the aromatic region, indicating that the lignin is G-unit enriched. The predominance of peaks in β-*O*-4′ substructure in the regenerated lignin represents γ-acylation β-*O*-4 substructure-related signals, which implies lactic acid acylation. After lactic acid-based DES treatment, the interunit linkage of lignin fragments was changed. Comparing the two-dimensional spectra of lignin before and after degradation, a new signal (marked in black) was observed, possibly due to the addition of DES [18,41]. In addition, the enhanced signal of Cγ-Hγ in regenerated lignin suggests that acylation may occur between the γ-OH group of lignin and the COOH group of lactic acid.
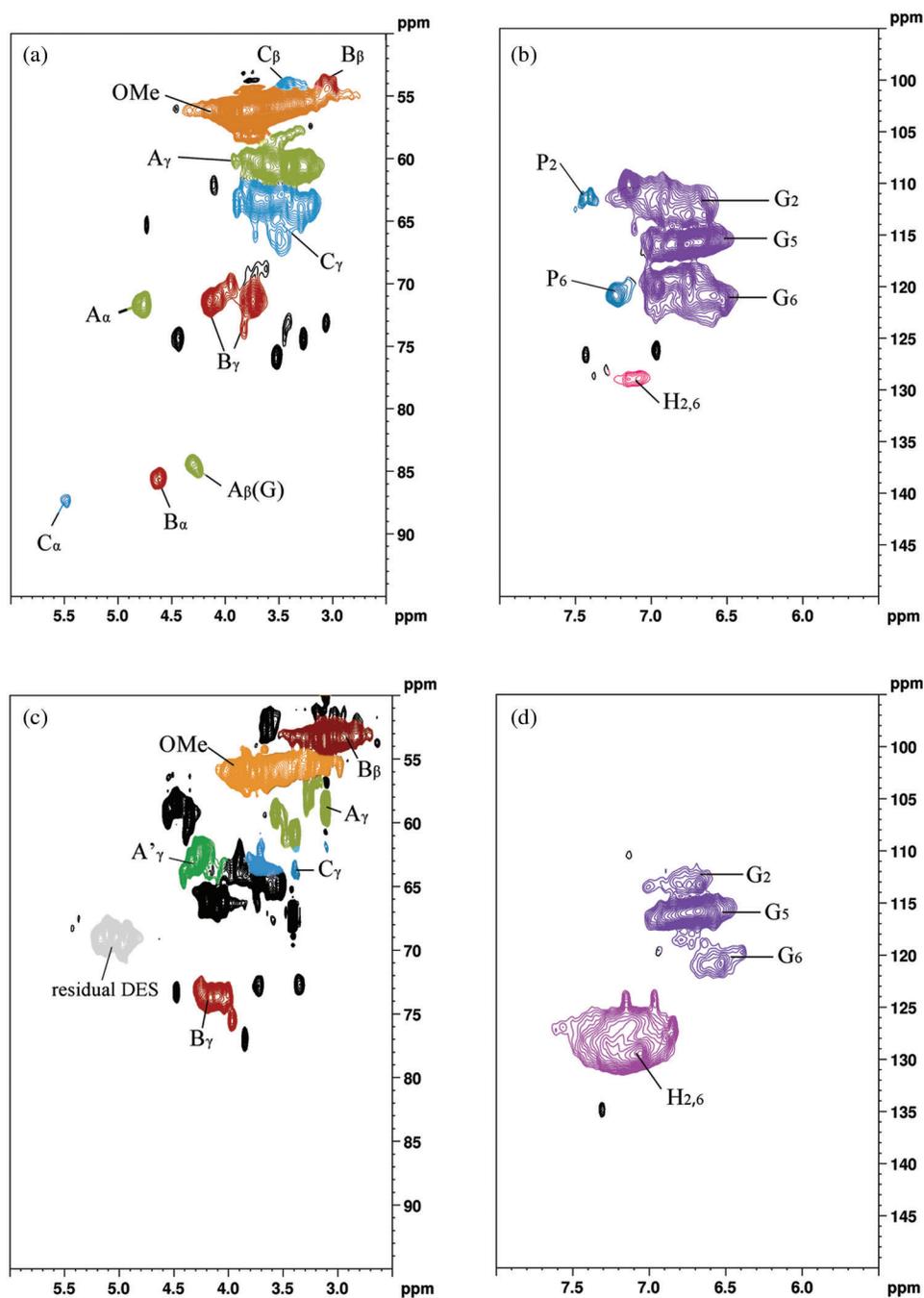
Figure 10: Two-dimensional nuclear magnetic resonance spectra of the original alkaline lignin (a, b) and the solid product after degradation (c, d)

3.10 GC-MS Analysis

To further investigate the degradation reaction of lignin in acidic deep eutectic solvents, the experiments were carried out by toluene extraction to obtain small molecule lignin degradation products from the recovered deep eutectic solvents after treatment at 180°C for 9 h. The composition was determined by GC-MS analysis, and the results are shown in Table 4.

Table 3: NMR assignments of major signals in 2D-HSQC NMR spectra of alkaline lignin and the regenerated lignin fractions [31,42]

Label	δ_C/δ_H (ppm)	Assignments
B_β	53.1/3.46	C_β–H_β in phenylcoumaran substructures (B)
C_β	53.5/3.05	C_β-H_β in β–β′ (resinol) substructures (C)
-OCH$_3$	56.4/3.70	C-H in methoxyls
A_γ	59.5/3.35–3.80	C_γ-H_γ in β–O–4′ substructures (A)
B_γ	62.3/3.76	C_γ-H_γ in phenylcoumaran substructures (B)
A'_γ	63.2/4.33–4.49	C_γ–H_γ in γ-acylated β-O-4′ substructures (A′)
C_γ	71.0/3.79–4.18	C_γ-H_γ in β–β′ resinol substructures (C)
A'_β(G)	80.8/4.62	C_β-H_β in β–O–4′ linked to G (A′)
A_β(G/H)	83.9/4.29	C_β–H_β in β–O–4′ substructures linked to G and H units (A)
C_α	84.9/4.64	C_α-H_α in β–β′ resinol substructures (C)
B_α	86.8/5.48	C_α-H_α in phenylcoumaran substructures (B)
G_2	111.0/6.99	C_2-H_2 in guaiacyl units (G)
G_5	114.8/6.68	C_5-H_5 in guaiacyl units (G)
G_6	119.1/6.80	C_6-H_6 in guaiacyl units (G)
$H_{2,6}$	127.9/7.19	$C_{2,6}$-$H_{2,6}$ in p-hydroxyphenyl units (H)
P_2	110.1/7.25	(C_2-H_2) in methyl-substituted phenylcoumarone substructure
P_6	119.5/7.20	(C_6-H_6) in methyl-substituted phenylcoumarone substructure

Table 4: Main lignin-degraded compounds in DES extracted by toluene

Serial number	Retention time	Name	Chemical structure formula	Relative content
1	5.26	1,3-Dimethyl-benzene		6.20
2	5.33	p-Xylene		5.01
3	5.59	Ethylbenzene		1.35
4	11.67	Vanillin		0.67
5	13.21	Butyrovanillone		0.64
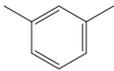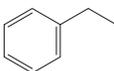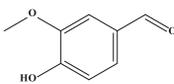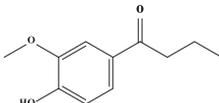
It can be found from Table 4 that the small molecular substances degraded by alkaline lignin are mainly composed of aldehydes, ketones, and phenolic substances. Among them, vanillin, and aromatic monomers were identified as the main lignin monomers in the depolymerization products. The identified products are mainly guaiac-based phenolics, consistent with 2D-HSQC analysis, indicating that the alkaline lignin is primarily composed of G units. Under the reaction temperature of 180°C and 9 h' reaction, the yield of

lignin monomer products can reach 14.67%, of which aromatic monomers occupy 12.56%. A small number of aldehydes and ketones are detected, such as vanillin (0.67%), butyrovanillone (0.64%), indicating the cleavage and oxidation of ether bonds occurred after the DES process. At the same time, the aromatic monomers in lignin were formed [18,31]. The overall yield of depolymerized compounds was not high due to the weak depolymerization effect of DES on lignin.

4 Conclusions

Using alkaline lignin as raw material, the effect of lactic acid and choline chloride on the degradation of lignin was studied. It was found that alkaline lignin could be degraded efficiently by DES in a relatively mild environment. By comparing phenolic hydroxyl groups, it was found that the content of phenolic hydroxyl groups in the supernatant after centrifugation was more than that of regenerated lignin, and smaller molecules of degradation products existed in the supernatant. It was found by FTIR that the ether bond in lignin molecules was broken and new hydroxyl groups were formed during the treatment of acidic DES. GPC showed that the polydispersity coefficient of degraded lignin decreased sharply, indicating that the degree of homogeneity of degraded lignin was improved. The hydrogen spectrum showed that it was mainly the fracture of the β-O-4 bond. XPS determination found that the DES treatment was accompanied by many oxidation reactions, such as the formation of ketones and esters. The recovery of the regenerated lignin samples was about 52%–77%, indicating that a portion of the lignin fraction was decomposed after treatment. Under a specific reaction time and temperature, a large number of β-O-4′ bonds and a small part of carbon-carbon bonds (i.e., β-β′, β-5′) are cleaved, resulting in an increase in phenolic OH groups and a decrease in molecular weight. The γ-OH in regenerated lignin can react with lactic acid for esterification under mild conditions. The process conditions of lignin depolymerization are mild, economical and feasible, and the degradation effect is ideal. It is hoped to further explore the degradation of lignin by adding some catalysts.

Conflicts of Interest: The authors declare that they have no conflicts of interest to report regarding the present study.

References

1. Radhika, N. L., Sachdeva, S., Kumar, M. (2022). Lignin depolymerization and biotransformation to industrially important chemicals/biofuels. *Fuel, 312(1),* 122935. DOI 10.1016/j.fuel.2021.122935.

2. Qu, X., Zhao, Y., Chen, Z., Wang, S., Ren, Y. et al. (2021). Thermoresponsive lignin-reinforced poly(ionic liquid) hydrogel wireless strain sensor. *Research, 12(1),* 9845482. DOI 10.34133/2021/9845482.

3. Singh, S. K., Dhepe, P. L. (2022). Alpha-, beta- and gamma-cellulose quantification and two-stage concentrated-dilute acid lignin recovery from three rice husks: Lignin characterization and depolymerization. *Waste and Biomass Valorization, 13(6),* 2963–2977. DOI 10.1007/s12649-022-01704-1.

4. Dong, J., Xu, W. H., Liu, S. B., Gong, Y. Z., Yang, T. et al. (2022). Lignin-derived biochar to support $CoFe_2O_4$: Effective activation of peracetic acid for sulfamethoxazole degradation. *Chemical Engineering Journal, 430(1),* 132868. DOI 10.1016/j.cej.2021.132868.

5. Zhang, X. S., Jian, W. B., Zhao, L., Wen, F. W., Chen, J. L. et al. (2022). Direct carbonization of sodium lignosulfonate through self-template strategies for the synthesis of porous carbons toward supercapacitor applications. *Colloids and Surfaces A: Physicochemical and Engineering Aspects, 636,* 128191. DOI 10.1016/j.colsurfa.2021.128191.

6. Wang, H. L., Ben, H. X., Ruan, H., Zhang, L. B., Pu, Y. Q. et al. (2017). Effects of lignin structure on hydrodeoxygenation reactivity of pine wood lignin to valuable chemicals. *ACS Sustainable Chemistry & Engineering, 5(2),* 1824–1830. DOI 10.1021/acssuschemeng.6b02563.

7. Kang, S. X., Bu, D. Q., Xue, L. Y., Wang, Q., Jiang, M. (2022). Degradation of lignin catalyzed by nanochannels solid acids in ionic liquid. *Polymer Degradation and Stability, 166(6),* 1–7. DOI 10.1016/j. polymdegradstab.2019.05.015.

8. Strüven, J. O., Meier, D. (2016). Hydrocracking of organosolv lignin in subcritical water to useful phenols employing various raney nickel catalysts. *ACS Sustainable Chemistry, 4(7),* 3712–3721. DOI 10.1021/ acssuschemeng.6b00342.

9. Sosa, F. H. B., Abranches, D. O., da Costa Lopes, A. M., Coutinho, J. A. P., da Costa, M. C., (2020). Kraft lignin solubility and its chemical modification in deep eutectic solvents. *ACS Sustainable Chemistry & Engineering, 8(50),* 18577–18589. DOI 10.1021/acssuschemeng.0c06655.

10. Das, L., Li, M., Stevens, J., Li, W., Pu, Y. et al. (2018). Characterization and catalytic transfer hydrogenolysis of deep eutectic solvent extracted sorghum lignin to phenolic compounds. *ACS Sustainable Chemistry & Engineering, 6(8),* 10408–10420. DOI 10.1021/acssuschemeng.8b01763.

11. Soares, B., Tavares, D. J. P., Amaral, J. L., Silvestre, A. J. D., Freire, C. S. R. et al. (2017). Enhanced solubility of lignin monomeric model compounds and technical lignins in aqueous solutions of deep eutectic solvents. *ACS Sustainable Chemistry & Engineering, 5(5),* 4056–4065. DOI 10.1021/acssuschemeng.7b00053.

12. Alvarez-Vasco, C., Ma, R., Quintero, M., Guo, M., Geleynse, S. et al. (2016). Unique low-molecular-weight lignin with high purity extracted from wood by deep eutectic solvents (DES): A source of lignin for valorization. *Green Chemistry, 18(19),* 5133–5141. DOI 10.1039/C6GC01007E.

13. Li, L., Wu, Z., Xi, X., Liu, B., Cao, Y. et al. (2021). A bifunctional brønsted acidic deep eutectic solvent to dissolve and catalyze the depolymerization of alkali lignin. *Journal of Renewable Materials, 9(2),* 219–235. DOI 10.32604/ jrm.2021.012099.

14. Wang, S. Z., Li, Y. H., Wen, X. F., Fang, Z. Q., Zheng, X. Z. et al. (2022). Experimental and theoretical study on the catalytic degradation of lignin by temperature-responsive deep eutectic solvents. *Industrial Crops and Products, 177,* 114430. DOI 10.1016/j.indcrop.2021.114430.

15. Tan, Y. T., Chua, A. S. M., Ngoh, G. C. (2020). Evaluation on the properties of deep eutectic solvent-extracted lignin for potential aromatic bio-products conversion. *Industrial Crops and Products, 154,* 112729. DOI 10.1016/j.indcrop.2020.112729.

16. Liu, X., Li, T. F., Wu, S. B., Ma, H., Yin, Y. (2020). Structural characterization and comparison of enzymatic and deep eutectic solvents isolated lignin from various green processes: Toward lignin valorization. *Bioresource Technology, 310(19),* 123460. DOI 10.1016/j.biortech.2020.123460.

17. Wang, S. Z., Li, H. L., Xiao, L. P., Song, G. (2020). Unraveling the structural transformation of wood lignin during deep eutectic solvent treatment. *Frontiers in Energy Research, 8,* 48. DOI 10.3389/fenrg.2020.00048.

18. Shen, X. J., Chen, T. Y., Wang, H. M., Mei, Q. Q., Yue, F. X. (2020). Structural and morphological transformations of lignin macromolecules during bio-based deep eutectic solvent (DES) pretreatment. *ACS Sustainable Chemistry & Engineering, 8(5),* 2130–2137. DOI 10.1021/acssuschemeng.9b05106.

19. Katahira, R., Mittal, A., Mckinney, K., Chen, X., Tucker, M. P. et al. (2015). Base-catalyzed depolymerization of biorefinery lignins. *ACS Sustainable Chemistry & Engineering, 4(3),* 1474–1486. DOI 10.1021/acssuschemeng.5b01451.

20. Rover, M. R., Brown, R. C. (2013). Quantification of total phenols in bio-oil using the Folin-Ciocalteu method. *Journal of Analytical and Applied Pyrolysis, 104,* 366–371. DOI 10.1016/j.jaap.2013.06.011.

21. Lin, X., Liu, M., Chen, L., Lyu, Y. (2021). Preparation of phenolic compounds by selective depolymerization of alkali lignin from *Sinocalamus Oldhami* using composite alkali. *Transactions of China Pulp and Paper, 36(2),* 1–8. DOI 10.11981/j.issn.1000-6842.2021.02.01.

22. Ouyang, X., Tan, Y., Qiu, X. (2014). Oxidative degradation of lignin for producing monophenolic compounds. *Journal of Fuel Chemistry and Technology, 42(6),* 677–682. DOI 10.1016/S1872-5813(14)60030-X.

23. Long, J., Xu, Y., Wang, T., Yuan, Z., Shu, R. et al. (2015). Efficient base-catalyzed decomposition and in situ hydrogenolysis process for lignin depolymerization and char elimination. *Applied Energy, 141,* 70–79. DOI 10.1016/j.apenergy.2014.12.025.

24. Xue, L., Yan, L., Cui, Y., Jiang, M., Xu, X. et al. (2016). Degradation of lignin in ionic liquid with HCl as catalyst. *Environmental Progress & Sustainable Energy, 35(3),* 809–814. DOI 10.1002/ep.12276.

25. Provost, V., Dumarcay, S., Ziegler-Devin, I., Boltoeva, M., Trébouet, D. et al. (2022). Deep eutectic solvent pretreatment of biomass: Influence of hydrogen bond donor and temperature on lignin extraction with high β-O-4 content. *Bioresource Technology, 349(19),* 126837. DOI 10.1016/j.biortech.2022.126837.

26. Li, P., Ren, J., Jiang, Z., Huang, L., Wu, C. et al. (2022). Review on the preparation of fuels and chemicals based on lignin. *RSC Advances, 12(17),* 10289–10305. DOI 10.1039/d2ra01341j.

27. Li, W. X., Xiao, W. Z., Yang, Y. Q., Wang, Q., Chen, X. et al. (2021). Insights into bamboo delignification with acidic deep eutectic solvents pretreatment for enhanced lignin fractionation and valorization. *Industrial Crops and Products, 170,* 113692. DOI 10.1016/j.indcrop.2021.113692.

28. Liu, Y., Chen, W., Xia, Q., Guo, B., Wang, Q. et al. (2017). Efficient cleavage of lignin-carbohydrate complexes and ultrafast extraction of lignin oligomers from wood biomass by microwave-assisted treatment with deep eutectic solvent. *ChemSusChem, 10(8),* 1692–1700. DOI 10.1002/cssc.201601795.

29. Wu, M., Pang, J., Lu, F., Zhang, X., Che, L. et al. (2013). Application of new expansion pretreatment method on agricultural waste. Part I: Influence of pretreatment on the properties of lignin. *Industrial Crops and Products, 50,* 887–895. DOI 10.1016/j.indcrop.2013.08.047.

30. Lv, H., Yan, L., Zhang, M., Geng, Z., Ren, M. et al. (2013). Influence of supercritical CO_2 pretreatment of corn stover with ethanol-water as co-solvent on lignin degradation. *Chemical Engineering & Technology, 36(11),* 1899–1906. DOI 10.1002/ceat.201300183.

31. Hong, S., Shen, X. J., Sun, Z. H., Yuan, T. Q. (2020). Insights into structural transformations of lignin toward high reactivity during choline chloride/formic acid deep eutectic solvents pretreatment. *Frontiers in Energy Research, 8,* 573198. DOI 10.3389/fenrg.2020.573198.

32. Hiltunen, J., Kuutti, L., Rovio, S., Puhakka, E., Virtanen, T. et al. (2016). Using a low melting solvent mixture to extract value from wood biomass. *Scientific Reports, 6(1),* 32420. DOI 10.1038/srep32420.

33. Hong, S., Shen, X. J., Xue, Z., Sun, Z., Yuan, T. Q. (2020). Structure-function relationships of deep eutectic solvents for lignin extraction and chemical transformation. *Green Chemistry, 22(21),* 7219–7232. DOI 10.1039/D0GC02439B.

34. Rahimi, A., Ulbrich, A., Coon, J. J., Stahl, S. S. (2014). Formic-acid-induced depolymerization of oxidized lignin to aromatics. *Nature, 515(7526),* 249–252. DOI 10.1038/nature13867.

35. Ahuja, D., Kaushik, A., Chauhan, G. S. (2017). Fractionation and physicochemical characterization of lignin from waste jute bags: Effect of process parameters on yield and thermal degradation. *International Journal of Biological Macromolecules, 97,* 403–410. DOI 10.1016/j.ijbiomac.2017.01.057.

36. Brebu, M., Vasile, C. (2010). Thermal degradation of lignin–A review. *Cellulose Chemistry and Technology, 44(9),* 353–363. DOI 10.1007/s10086-010-1118-1.

37. Shen, X. J., Wen, J. L., Mei, Q. Q., Chen, X., Sun, D. et al. (2019). Facile fractionation of lignocelluloses by biomass-derived deep eutectic solvent (DES) pretreatment for cellulose enzymatic hydrolysis and lignin valorization. *Green Chemistry, 21(2),* 275–283. DOI 10.1039/C8GC03064B.

38. Awal, A., Sain, M. (2011). Spectroscopic studies and evaluation of thermorheological properties of softwood and hardwood lignin. *Journal of Applied Polymer Science, 122(2),* 956–963. DOI 10.1002/app.34211.

39. Wen, J. L., Xue, B. L., Sun, S. L., Sun, R. C. (2013). Quantitative structural characterization and thermal properties of birch lignins after auto-catalyzed organosolv pretreatment and enzymatic hydrolysis. *Journal of Chemical Technology and Biotechnology, 88(9),* 1663–1671. DOI 10.1002/jctb.4017.

40. Faleva, A. V., Kozhevnikov, A. Y., Pokryshkin, S. A., Falev, D. I., Shestakov, S. L. et al. (2020). Structural characteristics of different softwood lignins according to 1D and 2D NMR spectroscopy. *Journal of Wood Chemistry and Technology, 40(3),* 178–189. DOI 10.1080/02773813.2020.1722702.

41. Hong, S., Shen, X. J., Pang, B., Xue, Z. M., Cao, X. F. et al. (2020). In-depth interpretation of the structural changes of lignin and formation of diketones during acidic deep eutectic solvent pretreatment. *Green Chemistry, 22(6),* 1851–1858. DOI 10.1039/D0GC00006J.

42. Wen, J. L., Sun, S. L., Xue, B. L., Sun, R. C. (2015). Structural elucidation of inhomogeneous lignins from bamboo. *International Journal of Biological Macromolecules, 77,* 250–259. DOI 10.1016/j.ijbiomac.2015.03.044.